Reactions of halonorbornane and oxo-substituted derivatives with different anions by the electron transfer mechanism; redox catalysis in stabilized radicals†‡

Jorge G. Uranga and Ana N. Santiago*

Received (in Gainesville, FL, USA) 23rd September 2009, Accepted 5th April 2010
DOI: 10.1039/b9nj00503j

Reactions of 2-bromo-, 2-chloronorbornane, 3-chloronorbornan-2-one and 3-bromocamphor with Me_3Sn^-, Ph_2P^- or PhS^- ions were studied by an $S_{RN}1$ mechanism in liquid ammonia or DMSO. The results show that substrates having a carbonyl group facilitate electron transfer reactions, which are impeded in the absence of such a group. However, when the free radical formed is stabilized by conjugation, the coupling reaction decreases, causing a concomitant increase in the reduction product. Theoretical studies explain the observed reactivity on the basis of a mechanism involving reductive cleavage as a function of the π–σ interactions.

Introduction

1-Bromonorbornane (1-BrNor) and other bridgehead compounds react with nucleophiles by a mechanism involving radical nucleophilic substitution ($S_{RN}1$), which involves an inter-molecular electron transfer step (inter-ET).[1] However, chlorinated substrates are less reactive, or even unreactive, by this mechanism.[2] The final outcome of an inter-ET reaction for organic halides is the formation of radicals by dissociation of the C–halogen bond. It is known that the presence of π-electron acceptors facilitates this inter-ET pathway,[2] where the reductive cleavage can be exerted by a mechanism involving either a concerted-dissociative or stepwise mechanism, with radical anions (RAs) as intermediates, depending on the orbital interactions, which lead to different pathways (eqn (1)).[3]

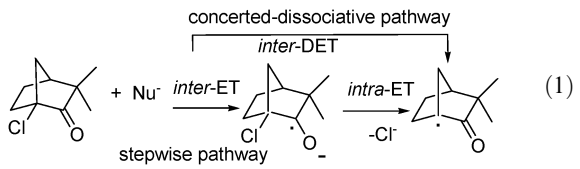

(1)

The reactivity of derivatives of bicyclo[2.2.1]heptan-2-one with nucleophiles has been previously studied. For instance, *endo*-bicyclo[2.2.1]heptan-2-on-3-yl-triflate reacts with NaOH, NaSCN or NaSPh, giving the corresponding *exo*-substituted products by the S_N2 mechanism.[4] Moreover, *exo*- and *endo*-bicyclo[2.2.1]heptan-2-on-3-yl-tosylates afford solvolysis in hexafluoroisopropanol.[5]

$S_{RN}1$ reactions in σ-chloro ketone-activated systems have been also reported. Reactions of these ketones with PhS^- involve both ionic and free radical ($S_{RN}1$) processes.[6] Furthermore, there is a recent report on the nucleophilic behavior of σ-keto radicals in addition reactions, depending on their conjugation.[7]

It is known that the oxo group may increase the initiation steps by redox catalysis in tertiary chlorides.[2] However, little is known of the behavior of radicals formed at a position α to the keto group, which can overlap with the oxo group. Thus, it is important to evaluate the stability of the radical formed, as well as its consequence on the global reaction pattern.

The main goal of this study was to evaluate the reactivity of the norbornyl system with nucleophiles by the $S_{RN}1$ mechanism. We also sought to assess the influence of the orientation of the oxo substituent in the global reaction. In addition, theoretical calculations are reported to further understand the reactivity and reaction mechanism.

Results and discussion

Reactions of compounds without an oxo substituent

exo-2-Chloronorbornane (2-ClNor) was unreactive with Ph_2P^- and PhS^- ions under irradiation (Table 1, experiments 1 and 6), whereas the bromide (*exo*-2-BrNor) reacted with Ph_2P^- and PhS^- ions using the same conditions (Table 1, experiments 2 and 7).

With Ph_2P^- ions, *exo*-2-BrNor afforded *exo*- and *endo*-2-norbornyldiphenyl phosphine (**1**) (92%, isolated as the oxide) (*exo*/*endo* = 19) (eqn (2)). This reaction did not occur in the dark and was partially inhibited by *p*-dinitrobenzene (*p*-DNB), a well-known inhibitor of $S_{RN}1$ reactions[1] (Table 1, experiments 2–5).

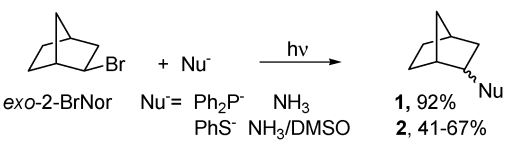

(2)

INFIQC, Departamento de Química Orgánica, Facultad de Ciencias Químicas, Universidad Nacional de Córdoba, Ciudad Universitaria, Córdoba 5000, Argentina. E-mail: santiago@fcq.unc.edu.ar; Fax: +54 351 4334170

† Dedicated to Professor Pelayo Camps García on occasion of his 65th birthday.

‡ Electronic supplementary information (ESI) available: NMR spectra, cartesian coordinates, reaction coordinates and thermodynamic quantities. See DOI: 10.1039/b9nj00503j

Table 1 Reactions of 2-halonorbornanes with nucleophiles for 180 min

Experiment	Substrate (M × 10^3)	Nucleophile (M × 10^3)	Conditions	Yield of substitution products (%)[a]
1	2-ClNor (4)	Ph_2P^- (4.1)	NH_3, *hν*	—
2	2-BrNor (4)	Ph_2P^- (4.1)	NH_3, *hν*	**1**, 92 (*exo*/*endo* = 19)
3	2-BrNor (4)	Ph_2P^- (4.1)	NH_3	—
4	2-BrNor (4)	Ph_2P^- (4.1)	NH_3, *hν*[b]	**1**, 77
5	2-BrNor (4)	Ph_2P^- (4.1)	NH_3, *hν*[c]	**1**, 13
6	2-ClNor (167)	PhS^- (833)	DMSO, *hν*	—
7	2-BrNor (83)	PhS^- (417)	DMSO, *hν*	**2**, 34
8	2-BrNor (83)	PhS^- (417)	DMSO	—
9	2-BrNor (167)	PhS^- (833)	DMSO, *hν*[d]	**2**, 41
10	2-BrNor (333)	PhS^- (1667)	DMSO, *hν*[d]	**2**, 67 (*exo*/*endo* = 4)

[a] Yields quantified by GLC using the internal standard method. [b] With *p*-DNB added (20 mol%). [c] With *p*-DNB added (50 mol%). [d] 240 min.

exo-2-BrNor reacted with PhS^- ions, yielding both *endo*- and *exo*-2-norbornylphenylsulfide (**2**) (34–67%, *exo*/*endo* = 4) (Table 1, experiments 7–10) (eqn (2)). However, this reaction did not occur in the dark, thus showing that a non-polar mechanism is involved (Table 1, experiment 8). Furthermore, if we compare the isomer ratio obtained with PhS^- ions (*exo*/*endo* = 4) to that observed with Ph_2P^- ions (*exo*/*endo* = 19), a better stereospecificity with Ph_2P^- ions is evident, probably due to the larger molecular size of the Ph_2P^- ion. A similar stereospecificity was found in the halogenation of norbornane by a free radical mechanism. In these reactions, the increase of stereospecificity was previously attributed to the relatively lower accessibility of the intermediate 2-norbornyl radical with bulkier reagents on the *endo* side.[8]

The absence of a reaction in the dark, as well as the inhibition observed during photostimulation in presence of *p*-DNB, suggests that these reactions occur by an $S_{RN}1$ mechanism (Scheme 1). When 2-BrNor receives one electron, it is fragmented at the C–Br bond by a dissociative electron transfer (DET) process. This affords radical intermediate **3**, which gives radical anion **4**$^{\bullet-}$ by a further reaction with the nucleophile (eqn (3)). Finally, **4**$^{\bullet-}$ yields the substitution product and **3**$^{\bullet}$ by DET to the substrate (eqn (4)), and **3**$^{\bullet}$ can continue the propagation chain.

We never observed the reduction product, only substitution products, indicating that **3**$^{\bullet}$ radicals react immediately with nucleophiles such as Ph_2P^- or PhS^- ions.

Reactions of bromo derivates with an oxo substituent

When *endo*-3-bromocamphor (**5a**) reacted with Me_3Sn^- or Ph_2P^- ions in liquid ammonia in the dark, only the reduction product was obtained (Table 2, experiments 1 and 3) (eqn (5)). The photostimulated reactions with these anions showed similar results.

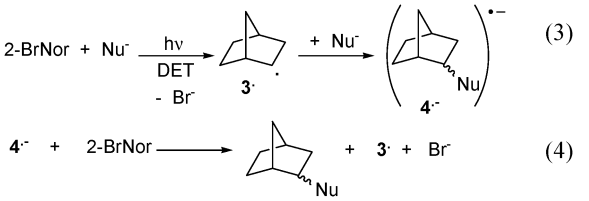

Scheme 1

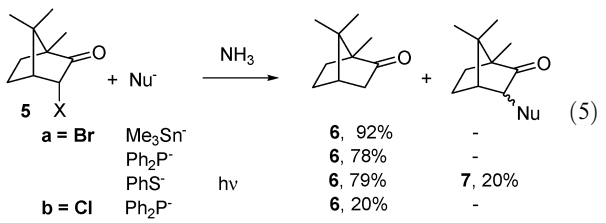

With Me_3Sn^- ions, the reduction showed little inhibition upon adding *p*-DNB (Table 2, experiment 2). These results might indicate that the reduction process yielded 70% by a halogen–metal exchange (HME) reaction, thus competing with a slow $S_{RN}1$ reaction.

When the Ph_2P^- ion was used as a nucleophile, both **5a** and **5b** gave a reduced product (78 and 20%, respectively). The reaction of **5b** with Ph_2P^- was inhibited by adding *p*-DNB, while the same reaction for **5a** was only partially inhibited (Table 2, experiments 3–6). The reaction of **5a** with Ph_2P^- was quenched by MeI, yielding less than 10% of two products (3-methyl-3-bromocamphor and 3-methylcamphor), arising from the methylation of α-keto-anions (Table 2). These results suggest that the reduction process proceeds by an electron transfer (ET) mechanism, as shown in Scheme 2. When **5** receives one electron, it fragments at the C–X bond through dissociative electron transfer (DET) to give radical intermediate **8**$^{\bullet}$, which then provides the reduction product by hydrogen abstraction from the solvent.

Me_3Sn^- and Ph_2P^- ions are common nucleophiles to the $S_{RN}1$ mechanism.[1] However, they do not react with radicals such as **8**$^{\bullet}$. The different reactivity of radicals **3**$^{\bullet}$ and **8**$^{\bullet}$ toward Ph_2P^- ions can be attributed to the stabilization of the latter by conjugation with the oxo group (see the Computational section). Further studies are in progress in order to understand the nature of the coupling reaction between **8**$^{\bullet}$ and nucleophiles.

When the PhS^- ion was used as a nucleophile, the photostimulated reaction of **5a** in either liquid ammonia or DMSO gave both reduction and substitution products (Table 2, experiments 7 and 8) (eqn (5)). In the dark, **5** was unreactive in DMSO (Table 2, experiment 9), showing that a non-polar mechanism is involved. The formation of the substitution product during the photostimulated reaction with PhS^- ions indicates that radical intermediate **8**$^{\bullet}$ coupled with PhS^- ions, surely in a similar pathway to that of 2-BrNor (Scheme 1).

Table 2 Reactions of 3-bromocamphors (**5**) with different nucleophiles[a]

Experiment	Substrate ($M \times 10^3$)	Nucleophile ($M \times 10^3$)	Conditions (time/min)	Yield of products (%)[b]	
				6	Substitution
1	**5a** (4)	Me_3Sn^- (4.1)	NH_3 (5)	92	—
2	**5a** (4)	Me_3Sn^- (4.1)	NH_3 (5)[c]	65	—
3	**5a** (4)	Ph_2P^- (4.1)	NH_3 (15)	78[d]	—
4	**5a** (4)	Ph_2P^- (4.1)	NH_3 (15)[e]	43[d]	—
5	**5b** (4)	Ph_2P^- (4.1)	NH_3(30)	20	—
6	**5b** (4)	Ph_2P^- (4.1)	NH_3 (30)[c]	—	—
7	**5a** (4)	PhS^- (12)	NH_3, *hν* (180)	79	**7**, 20
8	**5a** (25)	PhS^- (75)	DMSO, *hν* (180)	78	**7**, 22
9	**5a** (25)	PhS^- (75)	DMSO (180)	—	—

[a] The reactions were quenched with MeI. [b] Yields quantified by GLC by the internal standard method. [c] With *p*-DNB added (100 mol%). [d] 3-Methyl-3-bromocamphor and 3-methylcamphor were found in 2–10 and 3–7% yield, respectively. [e] With *p*-DNB added (50 mol%).

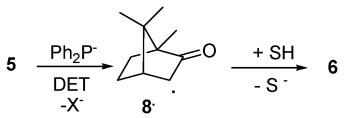

Scheme 2

Considering the formation of the reduction product in these reactions, it is evident that radical **3•** reacted with PhS^- ions faster than radical **8•**.

Reactions of chloro derivates with an oxo substituent

2-ClNor was unreactive in a photostimulated reaction with PhS^- ions in DMSO (Table 1, experiment 6). However, as previously mentioned, the reactivity could be increased when the chlorinated compound had an oxo-substituent.

In liquid ammonia, the photostimulated reaction of a mixture (1 : 1) of *endo*- and *exo*-3-chloro-2-norbornanone (**9**) with PhS^- afforded substitution products (**11**, *endo* : *exo*; 1.5 : 1) from low to moderate yields (0–61%) (Table 3, experiments 1–6). The same reaction in the dark did not proceed (Table 3, experiment 5) (eqn (6)).

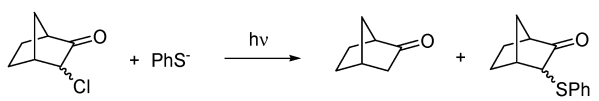

(6)

From the above-mentioned results, it is clear that the oxo group increases the initiation step but decreases the coupling reaction for chlorinated derivatives. The carbonyl group has a pronounced effect on the reduction potential of the radicals by more than 2 V.[9] This explains why the reduction pathway becomes much more favorable upon introducing an oxo functionality.

Finally, 1-chloro-3,3-dimethylbicyclo[2.2.1]heptan-2-one (**12**) is a bridgehead halide that is able to form a tertiary radical. It is known that **12** reacts with Ph_2P^- ions in liquid ammonia, giving substitution products in good yields under photostimulation (eqn (7)).[2] However, **12** failed to undergo a photostimulated reaction with PhS^- in DMSO (eqn (7)), probably due to problems in the initiation step. In order to analyze these experimental results, theoretical studies have been performed.

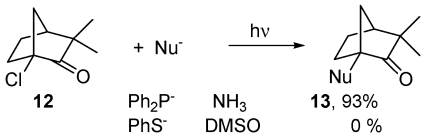

(7)

Theoretical studies of the chlorinated compounds

The coupling reactions between Ph_2P^- ions and radicals **14•** or **15•** could be performed according to the relative stability of the radicals and the substitution products.[10] In this sense, molecular orbital (MO) calculations were performed by considering the LUMOs of both neutral substitution products. In these cases, the LUMO energies were −0.0382 and −0.0369 eV for products derived from **14•** and **15•**, respectively (Fig. 1).

In addition, an important factor to be considered is $\Delta E\pi$, which represents the loss of π energy when conjugated radicals or conjugated nucleophiles couple. From the MO analysis, it is clear that the loss of π energy is higher for the substitution product arising from the secondary radical (from **15•** to the product in Fig. 1) than that corresponding to the product arising from the tertiary radical (from **14•** to the product in Fig. 1). The conjugation energy of 3.22 eV for secondary radical **15•** increases the energy gap necessary for the coupling, probably precluding this last reaction (see the ESI‡).

In the intermediate radical studied, the π-acceptor may be orthogonal and adjacent to the C–X bond (such as **14•** from **12**) or overlapped and adjacent to the C–X bond (as **15•** from **9**); the latter forming conjugated radicals. The conjugation of these radicals can be observed by their spin density distribution (Fig. 2A). Our calculations show that SOMOs corresponding to radicals **3•** or **14•** have higher spin densities on the carbon, whereas only radical **15•** has a spin density distributed between the carbon and the C═O bond.

Fig. 3 shows the B3LYP[11] profiles corresponding to the formation of different radicals from chlorinated compounds (such as 2-ClNor **9** and **12**), without including the methyl substituents in the calculations. These potential energy surfaces (PES), evaluated for the dissociation reaction, show

Table 3 Reactions of 3-chloro-2-norbornanone (**9**) and 1-chloro-3,3-dimethylbicyclo[2.2.1]heptan-2-one (**12**) with nucleophiles[a]

				Yield of products (%)[b]	
Experiment	Substrate (M × 10^2)	Nucleophile (M × 10^2)	Conditions (time/min)	Reduction	Substitution
1	**9** (0.4)	PhS^- (1.2)	NH_3, *hυ* (180)	**10**, 22	—
2	**9** (0.4)	PhS^- (2)	NH_3, *hυ* (240)	**10**, 26	**11**, 25
3	**9** (0.4)	PhS^- (2)	NH_3, *hυ* (330)	**10**, 34	**11**, 27
4	**9** (5)	PhS^- (25)	DMSO, *hυ* (180)	**10**, 78	**11**, 22
5	**9** (5)	PhS^- (25)	DMSO (180)	—	—
6	**9** (20)	PhS^- (100)	DMSO, *hυ* (240)	**10**, 27	**11**, 61[c]
7	**12** (20)	PhS^- (100)	DMSO, *hυ* (240)	—	—

[a] The reactions were quenched with MeI. [b] Yields based on substrate concentration, quantified by GLC using the internal standard method with adamantan-2-one as the reference. [c] The *endo*/*exo* ratio was 1.5.

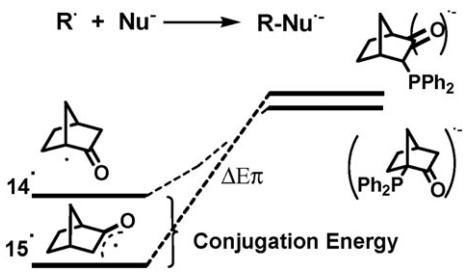

Fig. 1 A schematic profile of the coupling reactions of both conjugated (**15•**) and non-conjugated (**14•**) radicals toward the Ph_2P^- anion.

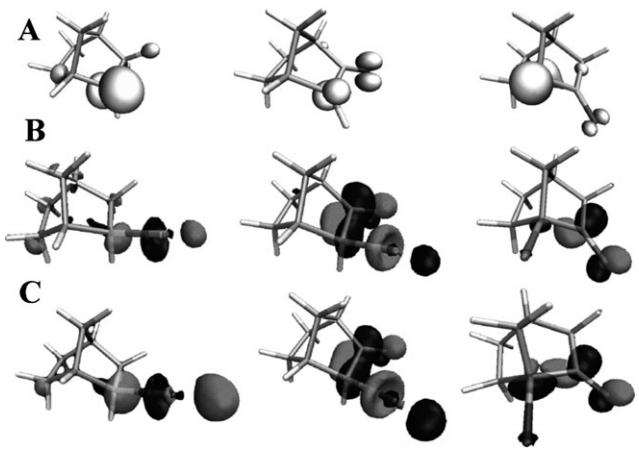

Fig. 2 A: The spin density on the carbon for radicals **3•**, **15•** and **14•**, respectively. B: Franck–Condon RAs for 2-ClNor **9** and **12**. C: Franck–Condon RAs for brominated analogues 2-BrNor **16** and **17**.

that a concerted dissociative pathway takes place, because no radical anions (RA) are observed on the anionic surface, which is in agreement with the experimental results observed with α-haloacetophenones.[12] Furthermore, Savéant[13] has proposed that an adiabatic estimation of the activation energy of the inter-DET can be evaluated from the crossing between the neutral and anionic surfaces for a given family of substrates with the same leaving group. Moreover, the relative energy of the anionic σ-surface, with respect to the neutral surface, provides information on the reductive cleavage (ΔE_{frag}). When the conjugated radical is formed, it modifies the energy of the anionic π- and σ-surfaces (— in Fig. 3), thereby producing a

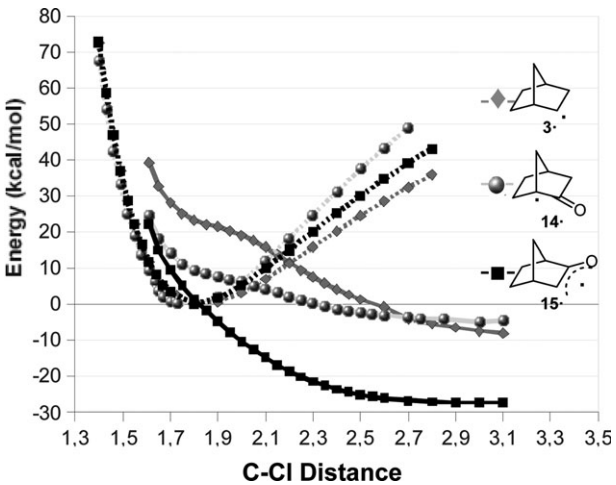

Fig. 3 Neutral (---) and anionic (—) profiles of 2-ClNor (**3•**, –◆–), **12** (**14•**, –●–) and **9** (**15•**, –■–). The neutral molecule is taken as zero energy.

crossing between the neutral and the anionic surfaces at lower energy.

Profiles for the brominated analogues 2-BrNor, 1-bromo-2-norbornanone (**16**) and 3-bromo-2-norbornanone (**17**) follow a similar tendency to the corresponding chlorinated compounds (Fig. 4). However, a significant difference observed with the brominated compounds is the enhancement in the stability of the anionic surface, which is largely due to the fact that bromide is a superior leaving group to chloride. However, it is difficult to make a straightforward comparison of energy surfaces belonging to the different leaving groups.[13] This is mainly because changes depend on several factors, not only the anionic curve stability. However, an important contribution that facilitates the inter-ET for brominated compounds is the shape of the crossing zone, being sharp for the chlorinated family and smooth for the brominated family. This effect could be attributed to both the stability of the anionic σ*-surface and the contribution of the lower bond dissociation energies (BDE) when the leaving group is Br^-.

Some of the relevant parameters calculated for the system are shown in Table 4. Compounds **12** (bridgehead) and 2-ClNor (no π-substitution) show less favorable electron affinities than **9**. This can be explained by considering that both the LUMO in the neutral structure and the SOMO in the

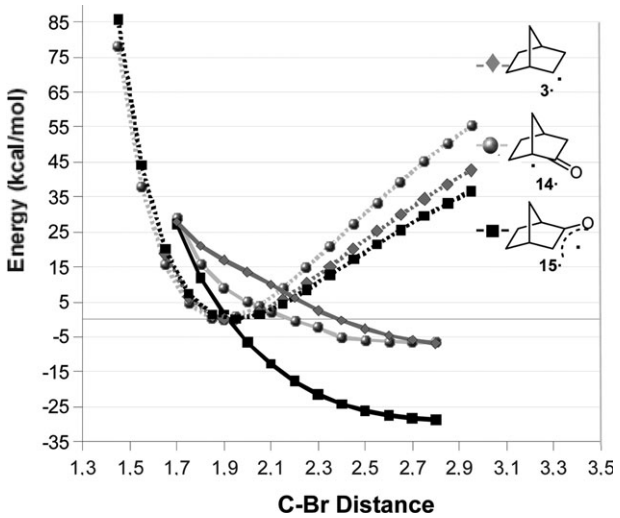

Fig. 4 Neutral (---) and anionic (—) profiles of 2-BrNor (**3**•, –◆–), **16** (**14**•, –●–) and **17** (**15**•, –■–). The neutral molecule is taken as zero energy.

reduced form are delocalized over a molecular orbital (MO) having π-σ* character, which increases the vertical electron affinity (VEA) for **9**. This indicates that the incoming electron is injected directly into a σ* C–Cl bond, with no formal *intra*-ET being necessary to break the bond (see Fig. 2B). Similar observations were made for SOMOs corresponding to brominated compounds, which showed a similar distribution (see Fig. 2C). However, the larger difference appears to be in the bridgehead compounds, where the σ* C–Br MO has a larger contribution in the SOMO, which seems to be the factor that enhances its VEA (as can be seen from Table 4).

The different thermodynamic parameters, such as ΔE_{frag} and the BDE, are in excellent agreement with the observed reactivity. No evidence of a sticky dissociative ET mechanism[14] was observed, since the interaction energies between the reduced fragments (D_p) for the oxo compounds (**9** and **12**) were quite similar.

The experimental reactivity of the observed initiation step (C–Cl fragmentation) is in agreement with a concerted dissociative cleavage of the halides, which depends on the global stability of the anionic σ-surface.

By considering the redox catalysis, **9** and **12** (oxo compounds) should be more reactive than 2-ClNor, since the oxo group is able to increase the electron affinity. However, in spite of this, **12** did not react with PhS^- ions due to the VEA of the isolated π system being not enough to ensure the formation of 2-oxo-1-norbornyl radicals (**14**•).

Conclusions

These results present new insights into understanding the effect of redox catalysis on the reactivity of chlorinated compounds. The presence of an oxo substituent facilitated the inter-ET pathway as it increased the electron affinity of the substrate, promoting the fragmentation of the C–Cl bond. However, the presence of the oxo substituent did not ensure the formation of a substitution product for the conjugated radical. Further studies on the influence of coupling conjugated radicals with different nucleophiles are necessary in order to fully understand the behavior of these radicals.

Experimental

General methods

Irradiation was conducted in a reactor equipped with two 400 W UV lamps emitting maximally at 350 nm (Philips Model HPT, water-refrigerated).

Materials

exo-2-Bromonorbornane, *exo*-2-chloronorbornane, *endo*- and *exo*-3-chloro-2-norbornanone, *endo*-3-bromocamphor, Me_3SnCl, Ph_3P, PhSH and potassium *t*-butoxide were commercially available and used as received. DMSO was distilled under vacuum and stored under molecular sieves (4 Å). Liquid ammonia was distilled under nitrogen and metallic Na, and used immediately.

General procedures

Photostimulated reactions of *exo*-2-BrNor with $^-SnMe_3$ ions in liquid ammonia. The following procedure is representative of these reactions. Me_3SnCl (1.2 mmol and Na metal (2.4 mmol) in small pieces were added to 250 mL of distilled ammonia until there was total decoloration between two consecutive additions. 20 min after the last addition, when no more solid was present, the $^-SnMe_3$ ions were ready for use (lemon yellow solution). The substrate *exo*-2-bromonorbornane (1 mmol) was added to the solution and the reaction mixture irradiated. Next, the reaction was quenched with an excess of ammonium nitrate and the ammonia allowed to evaporate. The residue was dissolved in water and then extracted with diethyl ether. The products were isolated by column chromatography. In the other experiments, the products were quantified by GLC using the internal standard method.

Photostimulated reactions of *exo*-2-BrNor with $^-PPh_2$ ions in liquid ammonia. The following procedure is representative of these reactions. PPh_3 (1.1 mmol) and Na metal (2.2 mmol) in

Table 4 Summary of results for the chlorinated and brominated substrates[a]

	2-ClNor	**9**	**12**	2-BrNor	**17**	**16**
VEA[b]	−0.974	−0.253	−0.611	−0.761	−0.011	−0.468
BDE[c] (RX → R• + X•)	75.98	65.68	87.02	74.4	63.69	85.11
ΔE_{frag}[d] (RX → R• + X$^-$)	−9.63	−19.93	1.17	−8.12	−18.83	2.59
D_p[e] (R•···X$^-$ → R• + X$^-$)	4.30	10.22	12.24	13.98	6.26	10.95

[a] Zero-point energy corrections were made at the 6-31 + G* level. [b] Gas phase vertical electron affinity (VEA) in eV. [c] Bond dissociation energy (BDE) in kcal mol^{-1}. [d] ΔE_{frag} in kcal mol^{-1}. [e] Interaction energy between dissociated fragments.

small pieces were added to 250 mL of distilled ammonia until no more solid was present, the Ph_2P^- ions now being ready for use (orange solution), and *t*-BuOH (1 mmol) was added to neutralize the amide ions formed. The substrate *exo*-2-bromonorbornane (1 mmol) was added to the solution and the reaction mixture irradiated. Next, the reaction was quenched with an excess of methyl iodide and the ammonia allowed to evaporate. The residue was dissolved in water and then extracted with diethyl ether. The products were isolated by column chromatography. In the other experiments, the products were quantified by GLC using the internal standard method.

Photostimulated reactions of *endo*- and *exo*-3-chloro-2-norbornanone with PhS^- ions in liquid ammonia. The following procedure is representative of these reactions. PhSH (5 mmol) and *t*-BuOH (5.1 mmol) were added to 250 mL of distilled ammonia, the PhS^- ions now being ready for use. The substrates *endo*- and *exo*-3-chloro-2-norbornanone (1 mmol) were added to the solution, and the reaction mixture irradiated. Next, the reaction was quenched with an excess of methyl iodide and the ammonia allowed to evaporate. The residue was dissolved in water and then extracted with diethyl ether. The products were isolated by column chromatography. In the other experiments, the products were quantified by GLC using the internal standard method.

Photostimulated reactions of *endo*- and *exo*-3-chloro-2-norbornanone with PhS^- ions in DMSO. The following procedure is representative of these reactions. To 5 mL of dry and de-gassed DMSO under nitrogen were added *t*-BuOK (5.1 mmol) and PhSH (5 mmol). After 15 min, *endo*- and *exo*-3-chloro-2-norbornanone (1.0 mmol) were added and the reaction mixture irradiated. The reaction was quenched with an excess of methyl iodide. The residue was dissolved in water and then extracted with diethyl ether. Finally, HNO_3 was added to the water phase up to pH 5–6. The water phase was then extracted with diethyl ether. The products were isolated by column chromatography. In similar experiments, the products were quantified by GLC using the internal standard method.

Reactions in the dark. The procedure was similar to that for the previous reaction, except that the reaction flask was wrapped with aluminium foil prior to substrate addition.

Inhibited reactions. The procedure was similar to that for the previous reaction, except that 20 mol% of *p*-DNB was added to the solution of nucleophile prior to substrate addition.

Isolation and identification of the products

2-Norbornyldiphenylphosphine oxide (1). ***exo***—GC-MS (EI^+) *m*/*z* (%): 296 (24), 295 (61), 230 (15), 229 (100), 202 (60), 201 (29), 155 (19), 125 (8), 77 (18). ***endo***—GC-MS (EI^+) *m*/*z* (%): 296 (39), 295 (15), 230 (18), 229 (100), 202 (89), 201 (23), 155 (14), 125 (8), 77 (16). ***exo***—^{1}H-NMR (400.16 MHz, $CDCl_3$, 25 °C): δ 1.17 (d, J = 9.8, 1H), 1.23–1.33 (m, 2H), 1.54–1.62 (m, 2H), 1.82–1.88 (m, 1H), 1.88–2.00 (m, 1H), 2.29 (t, J = 7.7, 1H), 2.34–2.37 (b, 1H), 2.49 (b, 1H), 7.52–7.39 (m, 6H) 7.70–7.84 (m, 4H). ^{13}C-NMR δ 28.67, 31.42 (d), 32.13 (d), 36.44 (CH, d), 37.30, 38.15, 39.89. ***exo*** and ***endo***—128.41, 128.44, 128.45, 128.52, 128.57, 128.62, 130.57 (d), 130.88, 130.91, 130.95, 130.97, 131.00, 131.03, 131.26, 131.29, 131.32, 131.34, 131.39 (d), 132.03 (d), 134.0 (d). ***endo***—^{1}H-NMR δ 1.21–1.32 (m, 2H), 1.34–1.40 (m, 1H), 1.48–1.53 (m, 2H), 1.68–1.77 (m, 2H), 2.27–2.31 (m, 1H), 2.35–2.39 (b, 1H), 2.36–2.40 (b, 1H), 2.55–2.60 (m, 1H) 7.52–7.39 (m, 6H) 7.70–7.84 (m, 4H). ^{13}C-NMR δ 25.23 (d), 29.21, 30.16, 37.58 (CH, d), 39.52 (d), 39.57, 41.28 (d). HRMS $[MH]^+$ calc. for $C_{19}H_{21}OP$ 297.1408; found: 297.1407.

2-Norborylphenylsulfide (2). ***exo***—GC-MS (EI^+) *m*/*z* (%): 206 (2), 205 (4), 204 (M^+) (33), 110 (24), 109 (8), 96 (9), 95 (100), 79 (14), 67 (34), 65 (11). ***endo***— GC-MS (EI^+) *m*/*z* (%): 206 (1), 205 (3), 204 (M^+) (20), 110 (20), 109 (6), 96 (7), 95 (100), 79 (6), 67 (29), 65 (9). ***exo***—^{1}H-NMR δ 1.03 (ddd J_1 = 2, J_2 = 6, J_3 = 12, 1H), 1.22–1.31 (m, 1H), 1.33–1.42 (m, 1H), 1.40–1.44 (t, J = 1.91 2H), 1.50–1.59 (m, 1H), 1.96–2.05 (m, 1H), 2.08–2.17 (m, 1H), 2.28 (t, J = 4.35, 1H), 2.38 (t, J = 2, 1H), 3.51–3.59 (m, 1H), 7,14 (tt, J_1 = 2, J_2 = 7, 1H), 7.22–7.29 (m, 2H), 7.32 (ddd, J_1 = 1.2, J_2 = 9, 2H). ^{13}C-NMR: δ 23.23, 29.81, 37.04, 38.16, 39.15, 40.84, 47.83, 125.52, 128.74, 129.53, 137.60. ***endo***—^{1}H-NMR: δ 1.12–1.32 (m, 1H), 1.32–1.47 (m, 3H), 1.48–1.64 (m, 1H), 1.65–1.74 (m, 1H), 1.76–1.84 (m, 1H), 2.30 (b, 1H), 2.32 (b, 1H), 3.16–3.22 (m, 1H), 7.14 (m, 1H), 7.22–7.29 (m, 2H), 7.32 (m, 2H). ^{13}C-NMR: δ 28.70, 28.91, 35.61, 36.52, 38.63, 42.33, 48.16, 125.52, 128.78, 128.97, 137.60. HRMS $[MH]^+$ calc. $C_{13}H_{16}S$ 205.1021; found: 205.1046.

1,7,7-Trimethyl-3-(phenylthio)bicyclo[2.2.1]heptan-2-one (7). ***exo***—GC-MS (EI^+) *m*/*z* (%): 260 (M^+) (34), 232 (5), 149 (100), 123 (35), 116 (16), 83 (8), 81 (11). ***endo***—GC-MS (EI^+) *m*/*z* (%): 260 (44), 232 (6), 150 (11), 149 (100), 147 (11), 134 (5), 123 (37), 116 (16), 115 (10), 109 (6), 81 (12), 65 (6), 55 (12). ***endo***—^{1}H-NMR: δ 0.92 (s, 3H), 0.96 (s, 3H), 1.03 (s, 3H), 1.7 (m, 4H), 2.0 (m, 1H), 2.28 (m, 1H), 3.92 (d, 1H), 7.33–7.17 (m, 3H), 7.43–7.56 (m, 2H). ^{13}C-NMR δ 9.68, 19.37, 19.67, 21.47, 30.81, 46.03, 48.66, 56.75, 58.64, 126.87, 130.06 (2C), 130.93 (2C), 135.72, 215.94. ***exo***—^{1}H-NMR δ 0.96 (s, 3H), 0.98 (s, 3H), 1.02 (s, 3H), 1.7 (m, 4H), 2.0 (m, 1H), 2.28 (m, 1H), 3.33 (d, 1H), 7.17–7.33 (m, 3H), 7.43–7.56 (m, 2H). ^{13}C-NMR δ 9.57, 19.37, 19.83, 21.51, 30.92, 46.7, 51.3, 57.71, 58.06, 126.57, 128.97 (2C), 130.10 (2C), 135.77, 216.89. HRMS $[MH]^+$ calc. for $C_{16}H_{20}OS$ 261.1313; found: 261.1308.

Computational procedures

These calculations were performed using Gaussian 03.[15] The characterization of stationary points was performed by Hessian matrix calculations. Exploration of the potential surface was carried out within the functional B3LYP,[12] and varying the selected coordinate with full optimization for the remaining degrees of freedom.

Acknowledgements

This work was supported in part by ACC, CONICET, SECYT and ANPCyT. J. G. U. gratefully acknowledges receipt of a fellowship from CONICET.

References

1 R. A. Rossi, A. B. Pierini and A. B. Peñéñory, *Chem. Rev.*, 2003, **103**, 71–167; A. N. Santiago, S. E. Martín and R. A. Rossi, in *Trends in Organic Chemistry*, ed. L. Menon, Council of Scientific Research Integration, Trivandrum, India, 2001, vol. 9, pp. 1–16; S. M. Palacios, R. A. Alonso and R. A. Rossi, *Tetrahedron*, 1985, **41**, 4147–4155; A. N. Santiago, A. E. Stahl, G. L. Rodríguez and R. A. Rossi, *J. Org. Chem.*, 1997, **62**, 4406–4411; M. Ahbala, P. Hapiot, A. Houman, M. Jouini, J. Pinson and J.-M. Savéant, *J. Am. Chem. Soc.*, 1995, **117**, 11488–11498.

2 A. N. Santiago, D. G. Morris and R. A. Rossi, *J. Chem. Soc., Chem. Commun.*, 1988, 220–221; A. N. Santiago, S. V. Iyer, W. Adcock and R. A. Rossi, *J. Org. Chem.*, 1988, **53**, 3016–3020; A. E. Lukach, D. G. Morris, A. N. Santiago and R. A. Rossi, *J. Org. Chem.*, 1995, **60**, 1000–1004; A. N. Santiago, K. Takeuchi, Y. Ohga, M. Nishida and R. A. Rossi, *J. Org. Chem.*, 1991, **56**, 1581–1584.

3 J. G. Uranga, D. M. A. Vera, A. N. Santiago and A. B. Pierini, *J. Org. Chem.*, 2006, **71**, 6596–99.

4 X. Creary and A. J. Rollin, *J. Org. Chem.*, 1979, **44**, 1798–1806.

5 H. Schneider, N. Becker, G. Schmidt and F. Thomas, *J. Org. Chem.*, 1986, **51**, 3602–3607.

6 G. A. Russell and F. Ros, *J. Am. Chem. Soc.*, 1982, **104**, 7349–2511; G. A. Russell and F. Ros, *J. Am. Chem. Soc.*, 1985, **107**, 2506–2511.

7 C. De Dobbeleer, J. Pospíil, F. De Vleeschouwer, F. De Proft and I. E. Markó, *Chem. Commun.*, 2009, 2142–2144.

8 E. C. Kooyman and G. C. Vegter, *Tetrahedron*, 1958, **4**, 382–392.

9 F. G. Bordwell, T. Gallagher and X. Zhang, *J. Am. Chem. Soc.*, 1991, **113**, 3495–3497; D. Occhialini, J. S. Kristensen, K. Daasbjerg and H. Lund, *Acta Chem. Scand.*, 1992, **46**, 474–481.

10 G. L. Borosky, A. B. Pierini and R. A. Rossi, *J. Org. Chem.*, 1992, **57**, 247–252; M. T. Baumgartner, A. B. Pierini and R. A. Rossi, *J. Org. Chem.*, 1993, **58**, 2593–2598; C. Galli, P. Gentili and Z. Rappoport, *J. Org. Chem.*, 1994, **59**, 6786–6795.

11 C. Lee, W. Yang and R. G. Parr, *Phys. Rev. B: Condens. Matter*, 1988, **37**, 785–789; A. D. Becke, *Phys. Rev. A: At., Mol., Opt. Phys.*, 1988, **38**, 3098–3100; B. Miehlich, A. Savin, H. Stoll and H. Preuss, *Chem. Phys. Lett.*, 1989, **157**, 200–206.

12 C. Andrieux, J. M. Savéant, A. Tallec, R. Tardivel and C. Tardy, *J. Am. Chem. Soc.*, 1997, **119**, 2420–2429.

13 J.-M. Savéant, in *Advanced Physical Organic Chemistry*, ed. T. T. Tidwell, Academic Press, New York, 2000, vol. 35, pp. 117–192.

14 A. Cardinale, A. Abdirisak, A. Gennaro, M. Robert and J. M. Savéant, *J. Am. Chem. Soc.*, 2002, **124**, 13533–13539; C. Ji, M. Ahmida, M. Chahma and A. Houman, *J. Am. Chem. Soc.*, 2006, **128**, 15423–15431.

15 M. J. Frisch, G. W. Trucks, H. B. Schlegel, G. E. Scuseria, M. A. Robb, J. R. Cheeseman, J. A. Montgomery, Jr., T. Vreven, K. N. Kudin, J. C. Burant, J. M. Millam, S. S. Iyengar, J. Tomasi, V. Barone, B. Mennucci, M. Cossi, G. Scalmani, N. Rega, G. A. Petersson, H. Nakatsuji, M. Hada, M. Ehara, K. Toyota, R. Fukuda, J. Hasegawa, M. Ishida, T. Nakajima, Y. Honda, O. Kitao, H. Nakai, M. Klene, X. Li, J. E. Knox, H. P. Hratchian, J. B. Cross, V. Bakken, C. Adamo, J. Jaramillo, R. Gomperts, R. E. Stratmann, O. Yazyev, A. J. Austin, R. Cammi, C. Pomelli, J. Ochterski, P. Y. Ayala, K. Morokuma, G. A. Voth, P. Salvador, J. J. Dannenberg, V. G. Zakrzewski, S. Dapprich, A. D. Daniels, M. C. Strain, O. Farkas, D. K. Malick, A. D. Rabuck, K. Raghavachari, J. B. Foresman, J. V. Ortiz, Q. Cui, A. G. Baboul, S. Clifford, J. Cioslowski, B. B. Stefanov, G. Liu, A. Liashenko, P. Piskorz, I. Komaromi, R. L. Martin, D. J. Fox, T. Keith, M. A. Al-Laham, C. Y. Peng, A. Nanayakkara, M. Challacombe, P. M. W. Gill, B. G. Johnson, W. Chen, M. W. Wong, C. Gonzalez and J. A. Pople, *GAUSSIAN 03 (Revision B.02)*, Gaussian, Inc., Wallingford, CT, 2004.

